

## A CORRELATION BETWEEN GALAXY LIGHT CONCENTRATION AND SUPERMASSIVE BLACK HOLE MASS

ALISTER W. GRAHAM<sup>1</sup>, PETER ERWIN<sup>2</sup>, N. CAON, I. TRUJILLO  
 Instituto de Astrofísica de Canarias, La Laguna, E-38200, Tenerife, Spain  
 agraham@ll.iac.es, erwin@ll.iac.es, ncaon@ll.iac.es, itc@ll.iac.es  
 submitted to *ApJL*, Sept 2001

### ABSTRACT

We present evidence for a strong correlation between the concentration of bulges and the mass of their central supermassive black hole ( $M_{\text{bh}}$ ) — more concentrated bulges have more massive black holes. Using  $C_{r_e}(1/3)$  from Trujillo, Graham, & Caon (2001b) as a measure of bulge concentration, we find that  $\log(M_{\text{bh}}/M_{\odot}) = 6.81(\pm 0.95)C_{r_e}(1/3) + 5.03 \pm 0.41$ . This correlation is shown to be marginally stronger (Spearman’s  $r_s = 0.91$ ) than the relationship between the logarithm of the stellar velocity dispersion and  $\log M_{\text{bh}}$  (Spearman’s  $r_s = 0.86$ ), and has comparable, or less, scatter (0.31 dex in  $\log M_{\text{bh}}$ , which decreases to 0.19 dex when we use only those galaxies whose supermassive black hole’s radius of influence is resolved and remove one well understood outlying data point). It would appear that the central black hole mass can be estimated from surface photometry alone, without the expensive addition of velocity dispersion determinations.

*Subject headings:* black hole physics, galaxies: fundamental parameters, galaxies: kinematics and dynamics, galaxies: nuclei, galaxies: photometry, galaxies: structure

### 1. INTRODUCTION

Observations over the last few years have established that supermassive black holes (SMBHs;  $\sim 10^6 - 10^9 M_{\odot}$ ) are a common, if not universal, feature at the centers of elliptical galaxies and the bulges of early-type spirals (Kormendy & Richstone 1995; Magorrian et al. 1998). Initial correlations between the masses of SMBHs and the absolute  $B$ -band luminosities of the host bulges<sup>3</sup> had a large scatter ( $\sim 0.5 - 0.6$  dex in  $\log M_{\text{bh}}$ , but see McLure & Dunlop 2001) which could not be accounted for by the assumed measurement errors. Subsequent studies uncovered a stronger correlation between the mass of the SMBH and the stellar velocity dispersion of the bulge, with considerably smaller scatter: only  $\sim 0.3$  dex in  $\log M_{\text{bh}}$  (Ferrarese & Merritt 2000; Gebhardt et al. 2000). Merritt & Ferrarese (2001a) argued that the observed scatter, for a select sample of 12 galaxies thought to have the most reliable SMBH mass estimates, was fully consistent with the measurement errors alone: that is, there may be no intrinsic scatter in the correlation. This clearly suggests that a strong cross-talk exists — or once existed — between the central black hole and its host bulge. The reasons for this, and the presumed formation mechanism are, however, not well understood, although many possibilities have been put forward (see, e.g., the discussion in Merritt & Ferrarese 2001b).

Recently, Graham, Trujillo, & Caon (2001) have shown that the central concentration of bulge light, measured within one effective half-light radius, positively correlates with the stellar velocity dispersion of the bulge. Following up on this, we present here, for the first time, a correlation between SMBH mass and bulge concentration, showing that more concentrated bulges have more massive SMBHs.

This correlation is found to be at least as strong as that between SMBH mass and stellar velocity dispersion, and may have less scatter. We suggest that the bulge concentration is certainly as significant a parameter, and one perhaps more revealing, than velocity dispersion (which presumably is a response to the underlying bulge mass distribution) for understanding the fueling and growth of central SMBHs. Furthermore, bulge concentration is easier to measure.

### 2. GALAXY DATA AND MEASUREMENTS

We began with the updated list of SMBH detections and mass estimates in the first two sections of Merritt & Ferrarese’s (2001b) Table 1. These black hole masses include a number of revised estimates from the “Nuker group” and STIS IDT team presented by Kormendy & Gebhardt (2001). This is an initial total of 30 galaxies, including the Milky Way. The only quantity that we have changed is the SMBH mass estimate for NGC 4374. Although this object appears in the list of galaxies with “reliable” SMBH mass estimates (because the black hole’s sphere of influence has been resolved), Maciejewski & Binney (2001) recently revised its mass estimate lower by a factor of four, after taking proper account of finite slit-width effects.

We searched the various public archives for high-quality  $R$ -band images<sup>4</sup> which were large enough to guarantee good sky subtraction and which had no central saturation. We found useful images for a total of 21 galaxies, primarily from the Isaac Newton Group and *Hubble Space Telescope* (HST) Archives; we also used images from Frei et al. (1996) and Hintzen et al. (1993), available via the NASA Extragalactic Database (NED). We were also able to use

<sup>1</sup> Department of Astronomy, Univ. of Florida, Gainesville, FL, USA

<sup>2</sup> Guest investigator of the UK Astronomy Data Centre

<sup>3</sup> By the term *bulge* we mean both elliptical galaxies and the bulges of spiral galaxies.

<sup>4</sup> For three galaxies, we used HST F814W images instead.

an unpublished image obtained with the WIYN Telescope<sup>5</sup> for NGC 3245, and the minor-axis near-infrared surface-brightness profile of the Milky Way published by Kent, Dame, & Fazio (1991), making a total of 23 galaxies with useable data.

A full discussion of the images for individual galaxies, along with reduction procedures and the extracted light profiles, analysis and model fitting for each galaxy will be presented in Erwin et al. (2001). Briefly, we fitted ellipses to the isophotes, allowing the position angle and ellipticity to vary with radius. The resulting light profiles were then fitted with a seeing-convolved<sup>6</sup> Sérsic (1968)  $r^{1/n}$  model. We modeled disk galaxy profiles with a combined (seeing-convolved) exponential disk and  $r^{1/n}$  bulge. For two galaxies with strong bars, we used the light profile derived from cuts along an axis perpendicular to the bar; this produced much better fits and avoided most of the bar contribution. The inner arc second of the profiles was generally excluded from the fit, since these regions are often dominated by relatively flat cores, bright nuclear disks, or nuclear point-sources (e.g., Rest et al. 2001, and references therein), none of which can be modeled with Sérsic profiles. We are thus measuring the overall concentration of the bulge, independent of any separate central stellar components like nuclear disks. Only two galaxies could not be successfully modeled. The final set of 21 galaxies with well-fitted profiles is given in Table 1.

We then computed the concentration of the best-fitting  $r^{1/n}$  models using the central concentration index first presented in Trujillo, Graham & Caon (2001b) and further developed in Graham et al. (2001). This index measures the light concentration within a bulge’s half-light radius ( $r_e$ ): it is the ratio of flux inside some fraction  $\alpha$  of the half-light radius to the total flux inside the half-light radius. For an  $r^{1/n}$  model, this index can be analytically defined as

$$C_{r_e}(\alpha) = \frac{\gamma(2n, b_n \alpha^{1/n})}{\gamma(2n, b_n)}, \quad (1)$$

where  $n$  is the shape parameter of the  $r^{1/n}$  model and  $b_n$  is derived numerically from the expression  $\Gamma(2n) = 2\gamma(2n, b_n)$  where  $\Gamma(a)$  and  $\gamma(a, x)$  are respectively the gamma function and the incomplete gamma function (Abramowitz & Stegun 1964). (This index *can* be measured empirically, without the use of Sérsic models, but for bulges in disk galaxies this would first require successful two-dimensional modeling and subtraction of disks, bars, etc.) The parameter  $\alpha$  can be any value between 0 and 1, and defines what level of concentration is being measured. Following Graham et al. (2001), we used a value of  $\alpha = 1/3$ . We did however explore a range of values, finding that  $\alpha = 1/3$  roughly produced the minimum vertical scatter in the  $\log M_{\text{bh}} - C_{r_e}(\alpha)$  correlation.  $C_{r_e}(1/3)$  is then simply the ratio of flux inside one-third of the half-light radius to the flux inside the entire half-light radius. (which is of course half the total bulge luminosity). The  $C_{r_e}(1/3)$

values are listed in the final column of Table 1. Because these values are analytically derived from the best-fitting Sérsic index  $n$ , the uncertainty in  $C_{r_e}(1/3)$  depends directly on the uncertainty in  $n$  and is derived by standard propagation of errors. Error estimates for  $n$  are based on the results of Caon, Capaccioli, & D’Onofrio (1993), who found a typical uncertainty of  $\sim 25\%$  when fitting with Sérsic profiles. For Sérsic values of  $n$  between 2 and 11, this corresponds to a 10-15% uncertainty in the bulge concentration.

For comparison with the known SMBH mass–velocity dispersion relation, we also list the velocity dispersions  $\sigma_c$  and corresponding errors for each galaxy; these are taken from Merritt & Ferrarese (2001b) and thus incorporate the equivalent-aperture correction described in Ferrarese & Merritt (2000). As Merritt & Ferrarese (2001a) showed, these values differ, on average, by only  $\sim 1\%$  from the  $\sigma_e$  values used by Gebhardt et al. (2000).

### 3. RESULTS

Correlations between SMBH mass and bulge concentration are presented in Figure 1; for comparison, we also show the correlations between SMBH mass and velocity dispersion for the same galaxies. We used the bisector linear-regression routine from Akritas & Bershady (1996) to fit a line to these correlations. This regression routine treats both variables equally, and allows for intrinsic scatter as well as measurement errors in the data; as Merritt & Ferrarese (2001a) point out, it is generally the best method to use when there are errors in both variables. Using the *orthogonal* regression analysis of Akritas & Bershady (1996) and the orthogonal distance regression routine FITEXY of Press et al. (1989) — alternate methods for data sets with errors in both variables — gave consistent results. We computed the Pearson correlation coefficient  $r$  and Spearman rank-order correlation coefficient  $r_s$ , both of which are given in Figure 1. The Spearman coefficient is preferred as it is more robust to outliers and does not presuppose a linear relation. The best linear fit to the whole sample is  $\log M_{\text{bh}} = 6.81(\pm 0.95)C_{r_e}(1/3) + 5.03 \pm 0.41$ .

Figure 1 shows that the correlation between black hole mass and bulge concentration is extremely good — as good as or better than that between black hole mass and velocity dispersion. In addition, the low  $\chi^2$  value of 0.82 suggests a scatter consistent with the measurement errors alone, implying negligible intrinsic scatter (as Ferrarese & Merritt 2000 claimed for the SMBH – velocity dispersion relation). This conclusion does, however, depend on how well determined the errors are; see Erwin et al. 2001.

Data points at the extreme ends of a correlation can be very useful for determining the true slope, due to the weight they lend, but by the same token they can heavily bias the data to produce a misleading slope if they themselves have not been well determined<sup>7</sup>. We have identified two such potential outliers<sup>8</sup> (NGC 7457 and NGC 6251) in

<sup>5</sup> The WIYN Observatory is a joint facility of the University of Wisconsin-Madison, Indiana University, Yale University, and the National Optical Astronomy Observatories.

<sup>6</sup> We used a Moffat function to describe the point-spread function; seeing full-width half-maxima were measured from stars in the individual images.

<sup>7</sup> This issue is discussed at length in Merritt & Ferrarese (2001a) for one galaxy in particular, namely, the Milky Way.

<sup>8</sup> These data points may be revealing negative curvature in the  $\log M_{\text{bh}} - C_{r_e}(1/3)$  relation, but we consider it premature to reach such a conclusion based on one data point at each end of the relation.

Figure 1a (see Section 4). We have repeated our analysis without them (bottom panels of Figure 1). In so doing, the  $\log M_{\text{bh}} - \log \sigma_c$  relation is even weaker than the  $\log M_{\text{bh}} - C_{r_e}(1/3)$  relation; it also has 27% more scatter in  $\log M_{\text{bh}}$ .

The list of galaxies in Merritt & Ferrarese (2001b), from which we constructed our sample, was subdivided according to whether or not the black hole’s sphere of influence had been resolved<sup>9</sup> Of the twenty-two “resolved” galaxies, we have images and useful fits for fourteen. We rederived the relations seen in Figure 1 using this smaller sample, and found that the strength of both correlations improved; for this subsample, both correlations appear equally strong (Figure 2).

A word of caution may be in order when comparing different measures of significance for these relations. The strength of a correlation itself — regardless of which function fits it — is best measured by the Spearman rank-order coefficient  $r_s$ . The  $\chi^2$  merit function for a *linear fit* to the data, the Pearson coefficient  $r$ , and the vertical scatter in  $\log M_{\text{bh}}$  all measure how well a straight line fits the data (or the logarithm of the data, as the case may be). In this vein, we note that while the strength of the  $\log M_{\text{bh}} - C_{r_e}(\alpha)$  correlation — as measured with the Spearman rank-order correlation coefficient — remains unchanged as  $\alpha$  and hence  $C_{r_e}(\alpha)$  vary, the  $\chi^2$  merit function steadily, and significantly, decreases as  $\alpha$  increases. This is easily understood from the way the absolute error in  $n$  propagates to an absolute error in  $C_{r_e}(\alpha)$ . Furthermore,

The  $\chi^2$  value depends on the size of the measurement errors: overestimating the errors will decrease the resulting  $\chi^2$ , even though the correlation is unchanged; underestimating the errors can produce a misleadingly large  $\chi^2$ . Thus, even though the  $\chi^2$  values for the  $M_{\text{bh}} - C_{r_e}(1/3)$  relation are either the same as (Figure 2) or much smaller than (Figure 1) those for the  $M_{\text{bh}} - \sigma_c$  relation, we do not take that as strong evidence that the  $M_{\text{bh}} - C_{r_e}(1/3)$  relation is better.

Ferrarese & Merritt (2000) argued that their optimal  $\log M_{\text{bh}} - \log \sigma_c$  relation had negligible intrinsic scatter; this led them to posit that, “Our results suggest that the stellar velocity dispersion may be the fundamental parameter regulating the evolution of supermassive BHs in galaxies.” All twelve of their ‘Sample A’ galaxies, from which this conclusion was reached, had an uncertainty of  $\pm 13\%$  on their central velocity dispersions, except for the Milky Way which had an uncertainty of  $\pm 20\%$ . If these uncertainties have been over-estimated it will result in an underestimate to the  $\chi^2$  value of the fit which may then lead one to wrongly conclude that there is no intrinsic scatter in the relation. The situation is identical if the  $\sim 10\text{-}15\%$  errors we assigned to the central concentration indices are too large.

To investigate the effect that decreasing the error estimates has on our correlations, we reperformed the regression analysis assuming only a 10% error on  $n$ , which translates to an impressively small 3% error in the derived concentration index when  $n = 8$  and a 6% error when  $n = 1$ . For the full galaxy sample, the slope of the best-fitting

line in the  $\log M_{\text{bh}} - C_{r_e}(1/3)$  diagram decreased slightly to  $6.12 \pm 0.78$  and  $\Delta \log M_{\text{bh}}$  changed to 0.30 dex. Removing NGC 6251 and NGC 7457, the slope was  $6.04 \pm 0.53$  and  $\Delta \log M_{\text{bh}}$  decreased to 0.24 dex.

The bulges studied here clearly have different luminosity distributions and, unless  $M/L$  varies with radius in a very contrived fashion, they also have different mass distributions from each other. If they did all possess the same universal structure, then the concentration index would be constant and identical for every bulge, which it is not. We will never have an accurate picture of bulge formation if we continue to pigeon-hole bulges into two simple classes, namely,  $r^{1/4}$  and exponential. Graham (1998) wrote “...one might expect [Sérsic’s]  $n$  to correlate with the size of the black hole predicted to be at the center of many elliptical galaxies.” Since  $C_{r_e}(1/3)$ , as defined in equation 1, is a monotonic function of the global shape parameter  $n$  (Trujillo et al. 2001b), the SMBH mass –  $C_{r_e}(1/3)$  correlation implies a correlation between SMBH mass and  $n$  as well. For the full galaxy sample, performing the bisector regression analysis on  $\log M_{\text{bh}}$  and  $\log n$  (assuming a 25% error in  $n$ ) gives  $\log M_{\text{bh}} = 2.93(\pm 0.43) \log n + 6.42 \pm 0.22$  with a scatter of 0.32 dex in  $\log M_{\text{bh}}$ . Excluding NGC 7457 and NGC 6251 gives  $\log M_{\text{bh}} = 3.00(\pm 0.17) \log n + 6.45 \pm 0.11$  with a scatter of only 0.25 dex. The strength of these correlations are of course equal to those shown in Figure 1a and c.

#### 4. DISCUSSION

Due to the weight that data points at the ends of a correlation can have on a line-of-best-fit, we have identified two outliers (NGC 7457 and NGC 6251) in Figure 1 which may be biasing the relation defined by the remaining bulk of data points. The most significant outlier in our relation is probably NGC 6251 in the top right of Figures 1a and 2a; it has both the highest black hole mass and the highest concentration index. There is reason to believe that its concentration index may be significantly in error. The best fitting Sérsic  $r^{1/n}$  model to this galaxy has  $n = 11$ , which means the outer profile of this model declines slowly with radius; the observed light-profile only extends to 1 model half-light radius. The larger the value of  $n$ , the closer the  $r^{1/n}$  model approaches a power-law in behavior — having infinite brightness and an infinite half-light radius (e.g., Graham et al. 1996), resulting in excessively high values of  $C_{r_e}(1/3)$ . Values of  $n$  greater than about 10 should thus be treated with caution. The outlying point (NGC 7457) in the lower left of Figure 1a is less easily dismissed, and may be a true outlier worthy of individual investigation<sup>10</sup> There is some evidence for a weak bar or lens in this galaxy (Michard & Marchal 1994). While we derived a light profile perpendicular to the major-axis of this feature, it does still have a finite width which can bias our Sérsic fit to the bulge, giving a spuriously large value for  $n$  and hence an over-estimation of the bulge concentration.

Although we cannot say which parameter ( $C_{r_e}(1/3)$  or  $\log \sigma$ ) is better, we can identify some of the advantages

<sup>9</sup> This is not necessarily a guarantee of accurate mass estimates: NGC 4374, which is near the top of Merritt & Ferrarese’s reliability ranking, recently had its mass readjusted by a factor of four (Maciejewski & Binney 2001).

<sup>10</sup> Interestingly, Tonry & Davis (1981) derived a stellar velocity dispersion for NGC 7457 of  $129 \text{ km s}^{-1}$  and Dressler & Sandage (1983) obtained a value of  $136 \text{ km s}^{-1}$ . If these values are a better measurement than the value of  $73 \text{ km s}^{-1}$  which has been used, one can see that this galaxy would also be an outlier in Figure 1b.

and disadvantages of each. Use of the concentration index for studies such as this may not be applicable to morphologically disturbed galaxies which may have undergone recent mergers or interactions (this could also influence the stellar velocity dispersion). Dominant cD galaxies that have acquired large extended envelopes can also be difficult to model and, depending on the extent of the accreted material, their concentration index may be heavily biased. The stellar velocity dispersion may, on the other hand, be a more stable quantity in such cases. Velocity dispersions have additionally been measured for numerous (mostly nearby) galaxies.

One obvious practical advantage that the concentration index has over stellar velocity dispersions is that images are far less expensive to acquire (in terms of telescope time) than stellar velocity dispersions; especially those at one effective radii. This is particularly important for studies of high-redshift galaxies. Second, use of the bulge concentration circumvents concerns that the SMBH may be influencing the luminosity-weighted nuclear velocity dispersion measurements (e.g. Wandel 2001). Similarly, while  $n$  and  $C_{r_c}$  are global parameters, velocity dispersion measurements are affected by: kinematical sub-structure at the centers of bulges, rotational velocity, seeing conditions, and aperture-size. It should also be noted, however, that the presence of bars, rings, and lenses within spiral galaxies can complicate the determination of the bulge concentration. A fourth advantage that the concentration index has is that it can be measured from photometrically uncalibrated images, it does not rely on distance measurements, redshift dependent corrections, or assumed mass-to-light ratios.

It appears that the formation mechanism(s) behind bulges must simultaneously determine their total luminosity, their eventual luminous structure (as measured by concentration index and Sérsic  $n$ ) and mass distribution, their stellar velocity dispersion, *and* the final mass of the central SMBH. Subsequent evolution, including the effects of mergers (once this process has neared completion), evidently preserves the above connections. To date, most models incorporating SMBHs have addressed their formation from the standpoint of the older  $M_{\text{bh}}-M_{\text{bulge}}$  relation (Haiman & Loeb 1998; Richstone et al. 1998; Silk &

Rees 1998; Blandford 1999; Kauffmann & Haehnelt 2000; Archibald et al. 2001; Umemura 2001); a few recent papers have offered possible explanations for the  $M_{\text{bh}}-\sigma$  correlation (Haehnelt & Kauffmann 2000; Adams, Graff, & Richstone 2001; Burkert & Silk 2001). We argue that a more complete understanding will be achieved when the correlation between SMBH mass and bulge concentration is also explained.

More luminous (massive) bulges have larger values of  $n$  (Trujillo et al. 2001b, and references therein), greater central concentrations, deeper gravitational potential wells with steeper central gradients (Ciotti 1991, Trujillo et al. 2001a), and more massive SMBHs. One might expect these characteristics to result in bulges which are better able to fuel and build their central black holes. It is however likely that the processes which shaped the galaxy and built the supermassive black hole operated in tandem.

Velocity dispersion measurements may simply be a somewhat more expensive tracer of the fundamental underlying mass distribution which can be more cheaply (in terms of telescope time) measured from galaxy light profiles.

We wish to thank Matthew Bershady for making available the linear regression code from Akritas & Bershady (1996).

Based on archival data obtained with the Isaac Newton Group of Telescopes operated on behalf of the UK Particle Physics and Astronomy Research Council (PPARC) and the Nederlandse Organisatie voor Wetenschappelijk Onderzoek (NWO) on the island of La Palma at the Spanish Observatorio del Roque de Los Muchachos of the Instituto de Astrofísica de Canarias.

Based on observations made with the NASA/ESA Hubble Space Telescope, obtained from the data archive at the Space Telescope Institute. STScI is operated by the association of Universities for Research in Astronomy, Inc. under the NASA contract NAS 5-26555.

This research has made use of the NASA/IPAC Extragalactic Database (NED) which is operated by the Jet Propulsion Laboratory, California Institute of Technology, under contract with the National Aeronautics and Space Administration.

## REFERENCES

- Adams, F.C. Graff, D.S., & Richstone, D.O. 2001, ApJ, 551, L31  
 Abramowitz M., Stegun I., 1964, Handbook of Mathematical Functions. Dover, New York, p.260  
 Archibald, E.N., Dunlop, J.S., Jimenez, R., Friaca, A.C.S., McLure, R.J., Hughes, D.H., 2001, MNRAS, submitted (astro-ph/0108122)  
 Akritas, M.G., & Bershady, M.A. 1996, ApJ, 470, 706  
 Blandford, R.D. 1999, in ASP Conf. Ser. 182, Galaxy Dynamics, ed. D. Merritt, J.A. Sellwood, & M. Valluri (San Francisco: ASP), 87  
 Burkert, A., & Silk, J. 2001, ApJ, 554, L151  
 Caon, N., Capaccioli, M., & D'Onofrio, M. 1993, MNRAS, 265, 1013  
 Ciotti, L. 1991, A&A, 249, 99  
 Ciotti, L., & Ostriker, J.P. 1997, ApJ, 487, L105  
 Ciotti, L., & Ostriker, J.P. 2001, ApJ, 551, 131  
 Dressler, A., & Sandage, A. 1983, ApJ, 265, 664  
 Erwin, P., Graham, A.W., Caon, N., & Trujillo, I. 2001, in prep  
 Ferrarese, L., & Merritt, D. 2000, ApJ, 539, L9  
 Frei, Z., Guhathakurta, P., Gunn, J. E., & Tyson, J. A. 1996, AJ, 111, 174  
 Gebhardt, K., et al. 2000, ApJ, 539, L13  
 Graham, A.W. 1998, PhD thesis, The Australian National University, p.72  
 Graham, A.W., Lauer, T.R., Colless, M.M., & Postman, M. 1996, ApJ, 465, 534  
 Graham, A.W., Trujillo, I., & Caon, N. 2001, AJ, 122, 1707  
 Haehnelt, M.G., & Kauffmann, G. 2000, MNRAS, 318, L35  
 Haehnelt, M.G., & Rees, M.J. 1993, MNRAS, 263, 168  
 Haiman, Z., & Loeb, A. 1998, ApJ, 503, 505  
 Hintzen, P., Angione, R., Talbert, F., Cheng, K.-P., Smith, E., Stecher, T. P. 1993, in The Evolution of Galaxies and Their Environment, (San Francisco: ASP), 38  
 Kauffmann, G., & Haehnelt, M. 2000, MNRAS, 311, 576  
 Kent, S.M., Dame, T., & Fazio, G. 1991, ApJ, 378, 131  
 Kormendy, J., & Richstone, D. 1995, ARA&A, 33, 581  
 Kormendy, J., & Gebhardt, K. 2001, in The 20th Texas Symposium on Relativistic Astrophysics, ed. H. Martel, & J.C. Wheeler, AIP, in press (astro-ph/0105230)  
 Maciejewski, W., & Binney, J. 2001, MNRAS, 323, 831  
 Madau, P., & Rees, M.J. 2001, ApJ, 551, L37  
 Magorrian, J., et al. 1998, AJ, 115, 2285  
 McLure, R.J. & Dunlop, J.S. 2001, MNRAS, submitted (astro-ph/0108417)  
 Merritt, D., & Ferrarese, L. 2001a, ApJ, 547, 140

- Merritt, D., & Ferrarese, L. 2001b, in *The Central Kpc of Starbursts and AGN: the La Palma Connection*, eds. J.H. Knapen, J.E. Beckman, I. Shlosman & T.J. Mahoney, (San Francisco: ASP), in press (astro-ph/0107134)
- Michard, R., & Marchal, J. 1994, *A&AS*, 105, 481
- Press, W.H., Flannery, B.P., Teukolsky, S.A., & Vetterling, W.T. 1989, *Numerical Recipes: The Art of Scientific Computing* (New York: Cambridge Univ. Press)
- Rest, A., et al. 2001, *AJ*, 121, 2431
- Richstone, D., et al. 1998, *Nature*, 395, A14
- Rix, H.-W., Carollo, C.M., & Freeman, K. 1999, *ApJ*, 513, L25
- Sérsic, J.-L. 1968, *Atlas de Galaxias Australes* (Cordoba: Observatorio Astronomico)
- Silk, J., & Rees, M.J. 1998, *A&A*, 331, L1
- Shapiro, S.L., & Teukolsky, S.A. 1988, in *Supermassive Black Holes*, ed. M. Kafatas, (Cambridge Univ. Press), 201
- Tonry, J., & Davis, M. 1981, *ApJ*, 246, 666
- Trujillo, I., Asensio Ramos, A., Rubiño-Martín, A., Graham, A.W., Aguerri, J.A.L., Cepa, J., & Gutiérrez, C.M. 2001a, *MNRAS*, submitted
- Trujillo, I., Graham, A.W., & Caon, N. 2001b, *MNRAS*, 326, 869
- Umemura, M. 2001, *ApJL*, in press (astro-ph/0108482)
- Wandel, A. 2001, *ApJ*, submitted (astro-ph/0108461)

TABLE 1  
GALAXY PARAMETERS

Galaxy	Revised Hubble Type	$\sigma_c$ (km s <sup>-1</sup> )	$M_{\text{bh}}$ (10 <sup>8</sup> M <sub>⊙</sub> )	$n$	$C_{r_e}(1/3)$
Ellipticals					
NGC 821	E6	196 ± 26	0.51±0.2	4.00	0.47 <sup>+0.04</sup> <sub>-0.06</sub>
NGC 3377	E5-6	131 ± 17	1.03 <sup>+1.6</sup> <sub>-0.41</sub>	3.50	0.44 <sup>+0.04</sup> <sub>-0.06</sub>
NGC 3379	E1	201 ± 26	1.35±0.73	4.64	0.49 <sup>+0.05</sup> <sub>-0.05</sub>
NGC 4261	E2-3	290 ± 38	5.4 <sup>+1.2</sup> <sub>-3.1</sub>	6.16	0.55 <sup>+0.04</sup> <sub>-0.06</sub>
NGC 4291	E	269 ± 35	1.54 <sup>+0.68</sup> <sub>-1.7</sub>	4.48	0.49 <sup>+0.04</sup> <sub>-0.06</sub>
NGC 4374	E1	286 ± 37	4.3 <sup>+3</sup> <sub>-1.7</sub>	4.97	0.51 <sup>+0.04</sup> <sub>-0.06</sub>
NGC 4473	E5	188 ± 25	1.026 <sup>+0.82</sup> <sub>-0.71</sub>	3.27	0.43 <sup>+0.04</sup> <sub>-0.06</sub>
NGC 4564	E6	153 ± 20	0.57 <sup>+0.13</sup> <sub>-0.17</sub>	2.06	0.34 <sup>+0.04</sup> <sub>-0.06</sub>
NGC 5845	E*	275 ± 36	3.52 <sup>+2.0</sup> <sub>-0.72</sub>	3.22	0.42 <sup>+0.05</sup> <sub>-0.05</sub>
NGC 6251	E	297 ± 39	5.9±2.0	11.0	0.65 <sup>+0.03</sup> <sub>-0.05</sub>
NGC 7052	E	261 ± 34	3.7 <sup>+2.6</sup> <sub>-1.5</sub>	4.56	0.49 <sup>+0.04</sup> <sub>-0.06</sub>
Bulges of Disk Galaxies					
NGC 1023	SB(rs)0 <sup>-</sup>	201 ± 14	0.39 <sup>+0.09</sup> <sub>-0.11</sub>	2.37	0.36 <sup>+0.05</sup> <sub>-0.05</sub>
NGC 2778 <sup>a</sup>	E	171 ± 22	0.20 <sup>+0.16</sup> <sub>-0.13</sub>	1.60	0.29 <sup>+0.04</sup> <sub>-0.05</sub>
NGC 2787 <sup>b</sup>	SB(r)0 <sup>+</sup>	210 ± 23	0.41 <sup>+0.04</sup> <sub>-0.05</sub>	1.96	0.33 <sup>+0.04</sup> <sub>-0.05</sub>
NGC 3031	SA(s)ab	174 ± 17	0.68 <sup>+0.07</sup> <sub>-0.13</sub>	3.23	0.42 <sup>+0.05</sup> <sub>-0.05</sub>
NGC 3245	SA(r)0	211 ± 19	2.1±0.5	4.04	0.47 <sup>+0.04</sup> <sub>-0.06</sub>
NGC 3384 <sup>b</sup>	SB(s)0 <sup>-</sup>	151 ± 20	0.185 <sup>+0.072</sup> <sub>-0.091</sub>	1.89	0.32 <sup>+0.04</sup> <sub>-0.05</sub>
NGC 4258 <sup>c</sup>	SAB(s)bc	138 ± 18	0.390±0.034	2.02	0.33 <sup>+0.04</sup> <sub>-0.05</sub>
NGC 4342 <sup>b</sup>	S0 <sup>-</sup>	261 ± 34	3.3 <sup>+1.9</sup> <sub>-1.1</sub>	5.12	0.51 <sup>+0.04</sup> <sub>-0.05</sub>
NGC 7457	SA(rs)0 <sup>-</sup>	73 ± 10	0.035 <sup>+0.027</sup> <sub>-0.017</sub>	1.81	0.31 <sup>+0.04</sup> <sub>-0.05</sub>
Milky Way <sup>d</sup>	Sb	100 ± 20	0.0295±0.0035	1.00	0.22 <sup>+0.03</sup> <sub>-0.04</sub>

<sup>a</sup>NGC 2778 is classified as an elliptical galaxy in the NASA Extragalactic Database (NED), but its light profile clearly indicates an S0 galaxy, with both an exponential disk and a central bulge; this interpretation is supported by the kinematical study of Rix, Carollo, & Freeman (1999).

<sup>b</sup>HST F814W image

<sup>c</sup>Thuan-Gunn  $r$  image

<sup>d</sup>2.4- $\mu\text{m}$  minor-axis profile from Kent, Dame, & Fazio (1991).

Note. — Galaxy types are from NED. Velocity dispersions and black hole masses from compilation in Merritt & Ferrarese (2001b), except SMBH mass for NGC 4374 (revised by Maciejewski & Binney 2001; updated errors from Kormendy & Gebhardt 2001). The central concentration  $C_{r_e}(1/3)$  of each bulge was measured from  $R$ -band images, except where otherwise noted, with a 25% uncertainty assumed for  $n$ .

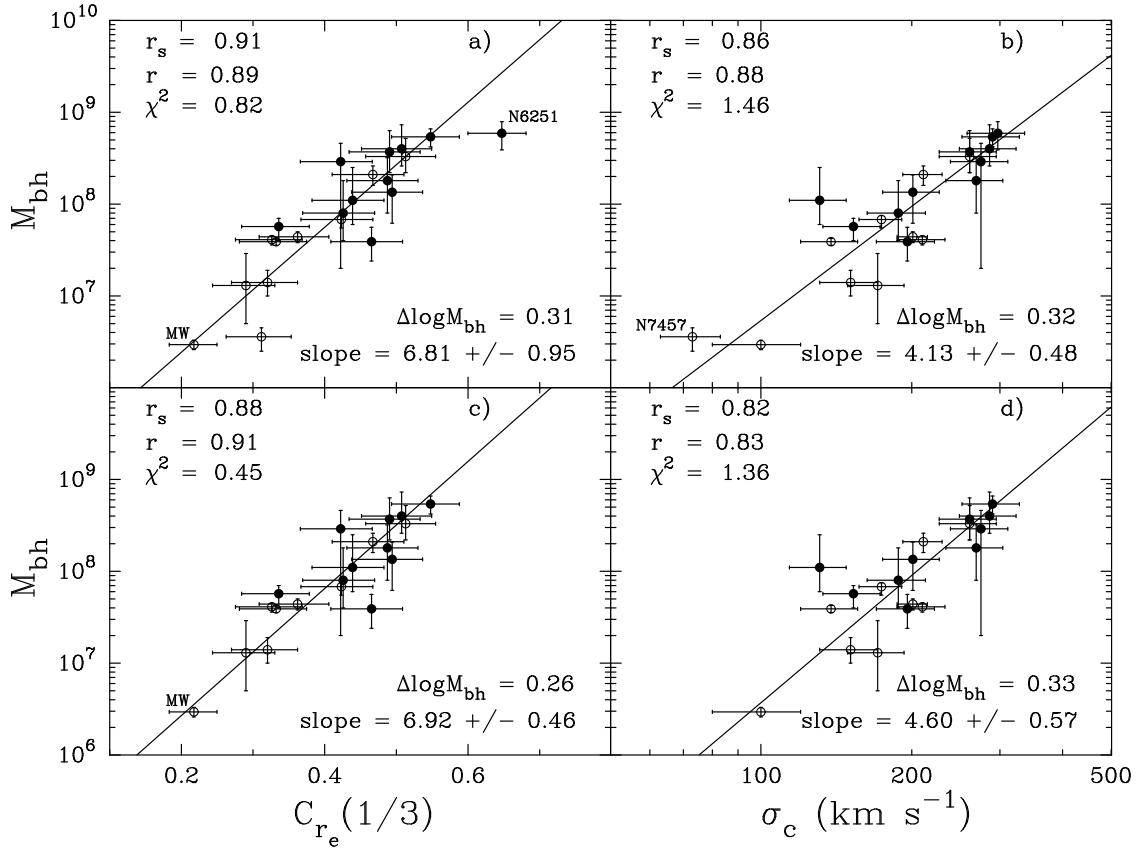


FIG. 1.— Correlations between supermassive black hole mass and a) bulge concentration and b) stellar velocity dispersion within  $r_e/8$ . c) and d) show the correlation after removing the two outlying galaxies (NGC 7457 and NGC 6251; see Section 3 and 4). The Milky Way (MW) has been indicated. The Spearman rank-order correlation coefficient  $r_s$  is given, as is the Pearson linear correlation coefficient  $r$ . The  $\chi^2$  merit function for a linear fit and the absolute vertical scatter  $\Delta \log M_{\text{bh}}$  are also given. Elliptical galaxies are denoted by filled circles, lenticulars and spirals by open circles.

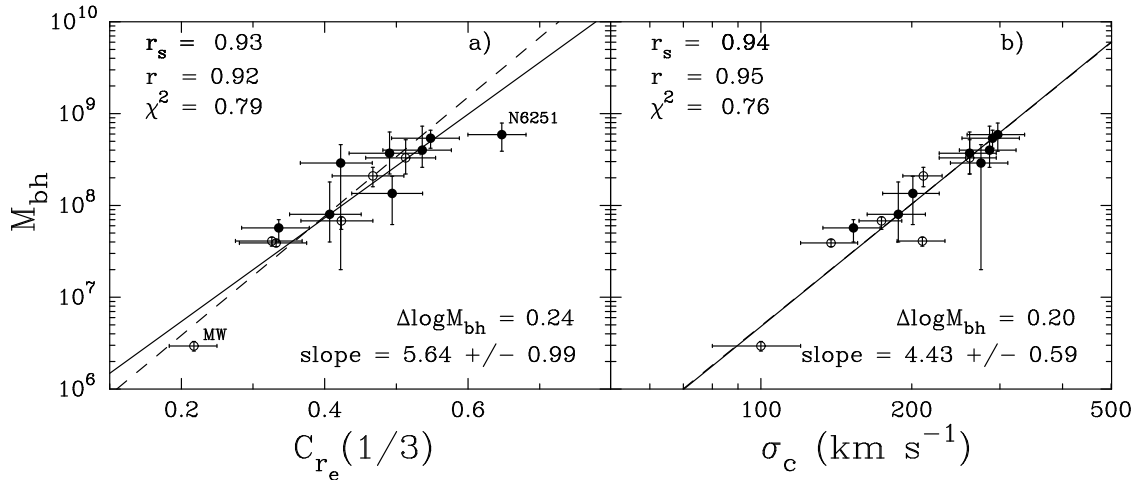


FIG. 2.— Same as Figure 1, except using only those galaxies with resolved SMBH spheres of influence (top section of Table 1, Merritt & Ferrarese 2001b). The dashed line shows the correlation after removing NGC 6251, as done in Figure 1. The slope to the dashed line in panel a) is  $6.49 \pm 0.78$  and has a vertical scatter of 0.19 dex. The slope to the dashed line in panel b) is  $4.41 \pm 0.66$  with a vertical scatter of 0.20 dex.